THE JOURNAL OF PHYSICAL CHEMISTRY B

Article

pubs.acs.org/JPCB

Charge Transfer in Single Chains of a Donor–Acceptor Conjugated Tri-Block Copolymer

Emma N. Hooley,[†] David J. Jones,[†] Neil C. Greenham,[‡] Kenneth P. Ghiggino,*[,†] and Toby D. M. Bell*[,§]

[†]School of Chemistry, University of Melbourne, Parkville, Victoria 3010, Australia

[‡]Cavendish Laboratory, University of Cambridge, J. J. Thomson Avenue, Cambridge CB3 OHE, United Kingdom

[§]School of Chemistry, Monash University, Clayton, Victoria 3800, Australia

Supporting Information

ABSTRACT: The photophysics of a conjugated triblock copolymer comprising poly(9,9-dioctylfluorene-*co*-bis-N,N′-(4-methylphenyl)-bis-N,N′-phenyl-1,4-phenylenediamine) (PFM) electron donor and poly(4-(9,9-dioctyl-9*H*-fluoren-2-yl)benzo[*c*][1,2,5]-thiadiazole) (F8BT) electron acceptor blocks has been studied in solution, in films, and as single chains. While an additional long-wavelength emission apparent in neat films of the copolymer is attributed to interchain exciplex formation, no such long-wavelength emission is apparent in solution or from single molecules. However, in these cases, time-resolved fluorescence measurements indicate the presence of a delayed fluorescence. The kinetics of the delayed emission can be interpreted in terms of an equilibrium between a locally excited and a charge-transfer state at the interface of the copolymer block components. Rate constants and thermodynamic quantities associated with these processes have been evaluated. The single-molecule results allow the assignment of an intramolecular charge-transfer state in an isolated conjugated block copolymer chain.

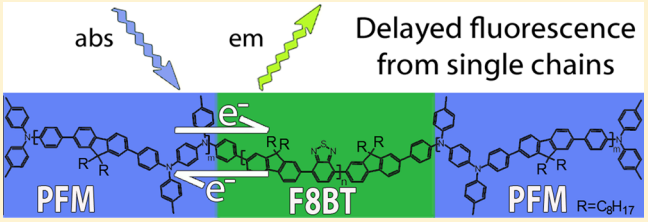

INTRODUCTION

Polymers containing sequences of π-conjugation along the polymer backbone have attracted considerable interest because their combination of optical and electronic properties lends them to applications in organic photovoltaics[1,2] and organic light-emitting diodes.[3] Following photoexcitation these "conjugated polymers" can act as electron donors in the presence of other small-molecule or polymer electron acceptors, and this provides the basis for the use of these materials in organic solar cells.[4,5] Photoexcitation at first creates a bound electron–hole pair, or exciton, that can migrate over short distances in the conjugated polymer. To achieve photocurrent generation, the exciton needs to encounter a suitable electron acceptor to ultimately yield complete separation of the charges that can then migrate independently to the appropriate electrode. Thus, efficient solar cell performance requires both effective charge transfer and separation at the interface between the donor and acceptor species as well as a continuous pathway for the unbound charges to travel to the device electrodes. Bulk heterojunction solar cells made up of blends of the donor and acceptor materials go some way to solving these problems; however, careful control over the morphology of the film components is necessary.[6,7]

To impose an element of control over the morphology of the active layer in organic photovoltaic devices, block copolymers consisting of electron donor and acceptor blocks have been investigated[8−11] and show some promise in optimizing charge separation. As each polymer chain contains a donor–acceptor interface, intramolecular charge transfer (CT) can occur. Including donor–acceptor interfaces within a single polymer chain ensures close contact between donor and acceptor blocks and reduces the influence of blend morphology on the extent and position of the donor–acceptor interface. Utilizing self-assembly behavior, a structured environment can be provided for the separated, unbound charges to travel freely to the electrodes.

Both intramolecular CT and intermolecular CT are possible when an appropriate lower-energy CT state (with respect to the locally excited state) exists and can be populated. Nonradiative recombination is a common fate of CT states; however, radiative relaxation resulting in emission from the CT state is also possible. Polymer blend[12,13] and small molecule studies[14,15] have shown that, given an appropriate energy arrangement of electronic states involved, photoinduced electron-transfer processes can result in an equilibrium between the locally excited (LE) singlet state and the CT state. The position of the equilibrium is often dependent on the local environment, which can control the energetics.[16] While the CT state has been studied in donor–acceptor conjugated polymers,[17−19] it has not been reported at the single-chain level. Back electron transfer from fully charge separated species can lead to reformation of the ground state; however, when the

Special Issue: John R. Miller and Marshall D. Newton Festschrift

Received: October 27, 2014
Revised: November 23, 2014
Published: November 24, 2014

   dx.doi.org/10.1021/jp510769p | J. Phys. Chem. B 2015, 119, 7266–7274

Chart 1. Chemical Structure of the PFM-F8BT-PFM Triblock Copolymer and PFM and F8BT Homopolymers

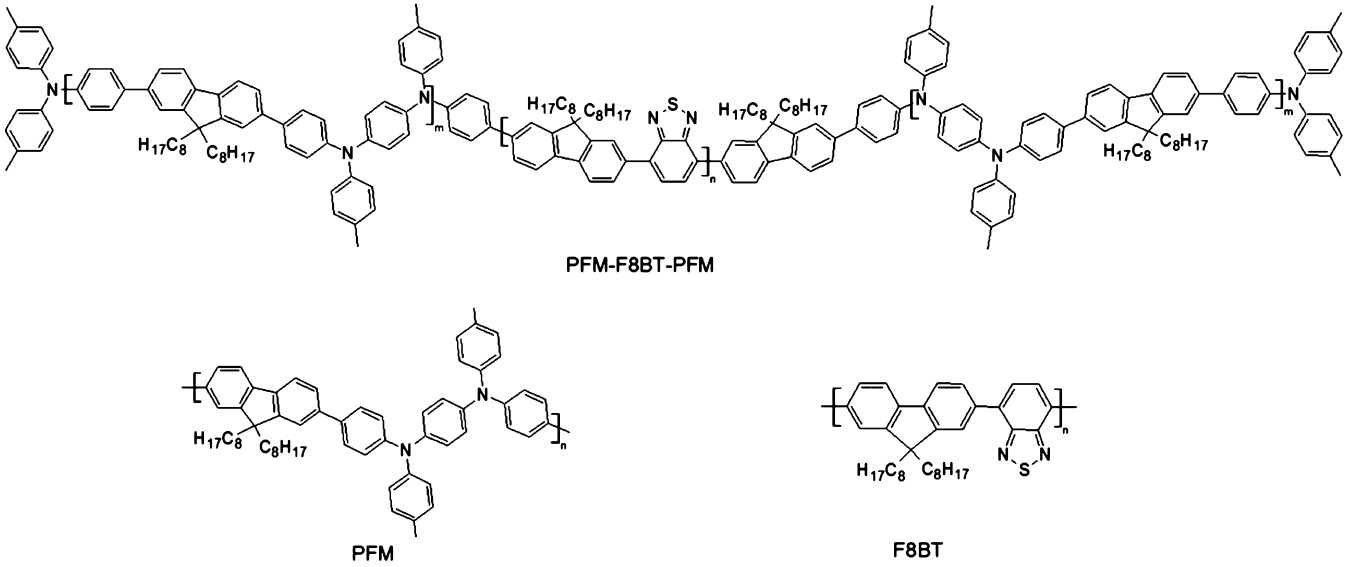

energy levels are appropriate and the LE state and CT state are in equilibrium, a delayed fluorescence can occur facilitated by thermal back transfer from the CT state to regenerate the LE state.

In this work, we report on the photophysics of a donor−acceptor triblock copolymer PFM-F8BT-PFM, consisting of electron donor PFM (poly(9,9-dioctylfluorene-*co*-bis-N,N′-(4-methylphenyl)-bis-N,N′-phenyl-1,4-phenylenediamine)) and electron acceptor F8BT (poly[(9,9-di-n-octylfluorenyl-2,7-diyl)-*alt*-(benzo[2,1,3]thiadiazol-4,8-diyl)) (Chart 1). This donor−acceptor block copolymer has been used as the active layer in photovoltaic devices[20] where it outperformed a simple 2:1 blend of PFM:F8BT by a factor of 3 in terms of power conversion efficiency of the devices. In the present work, the observation of a delayed fluorescence component in solution, neat film, and in single chains is attributed to the presence of an intrachain charge-transfer state in the block copolymer.

EXPERIMENTAL SECTION

A central poly(4-(9,9-dioctyl-9*H*-fluoren-2-yl)benzo[*c*][1,2,5]-thiadiazole) (F8BT) electron-accepting block was synthesized by Suzuki condensation followed by end-capping with trimethylsilylpheny groups and reaction with ICl. The block size was controlled by monomer ratio followed by removal of low molecular weight oligomers via Soxhlet extraction with ethyl acetate leaving a polymer with (M_n = 21 200, M_w = 32 000, M_w/M_n = 1.51). Chain extension with *N*1-(4-(7-(4-iodophenyl)-9,9-dioctyl-9*H*-fluoren-2-yl)phenyl)-N^1,N^4-di-*p*-tolylbenzene-1,4-diamine under Buchwald−Hartwig conditions, followed by end-capping with bromotoluene, resulted in the formation of the triblock copolymer PFM-F8BT-PFM. The triblock copolymer had a PFM:F8BT weight ratio of 1:1 (M_n = 43 500, M_w = 56 400, M_w/M_n = 1.30). Synthetic polymerization, characterization details, and photovoltaic device performance of this block copolymer have been published elsewhere.[20,21]

Absorption spectra were recorded using a Cary 50 Bio ultraviolet−visible (UV−vis) spectrophotometer (Agilent) with solvent baseline subtraction, and a Cary Eclipse Fluorimeter (Agilent) was used to measure solution emission spectra. Bulk samples were prepared using spectroscopic grade solvents (Aldrich) which were used as received. Fluorescence quantum yields in solution were determined from emission spectra corrected for the wavelength dependence of the detector efficiency by comparing the emission of PFM-F8BT-PFM against the standard disodium fluorescein in ethanol (Φ_{fl} = 0.79).[22] Degassed solutions where the maximum absorbance was kept below 0.1 were used to avoid oxygen quenching and inner filter effects.

Fluorescence lifetimes were determined by the method of time-correlated single-photon counting (TCSPC). Full details of the experimental setup and data analysis are published elsewhere.[23] Briefly, excitation was provided by a "white light" supercontinuum fiber laser source (Fianium SC-400−4-pp) operated at 5 MHz and 488 ± 5 nm light selected using a narrow bandpass filter (Chroma). Fluorescence was collected at 90° through a monochromator (Digikrom DK480) and focused onto an avalanche photodiode (APD) (IdQuantique Id-100). Data collection and photon arrival timing was achieved using a photon counting module (PicoQuant PicoHarp300) and transferred to a PC. Decay curves were analyzed by a least-squares fitting method based on the Levenberg−Marquardt algorithm using the TRFA Global Analysis program (Scientific Software Technologies Centre) taking into account the instrument response function (IRF). For film measurements, samples were prepared on clean glass coverslips and mounted on a confocal, inverted fluorescence microscope (Olympus IX71). Laser light was focused through a high numerical aperture objective (Olympus PSPlanApo 100X/1.4 NA), and fluorescence was collected through the same objective, separated from the excitation light by a dichroic filter (Chroma) and focused onto an APD (PicoQuant TauSPAD). Instrument response functions were measured from a scattering solution or from a clean, blank coverslip. Emission spectra from films were measured using the confocal microscope with the fluorescence emission directed through a spectrograph (Princeton Instruments Acton SP2150) and onto an electron multiplying CCD camera (Princeton Instruments ProEm512).

For single-molecule spectroscopy, samples were diluted to ~1×10^{-9} mol dm^{-3} of polymer by serial dilution in $CHCl_3$ (Aldrich) with the final dilution into a ~0.5% (w/w) solution of poly(methyl methacrylate) (PMMA) (Aldrich) in $CHCl_3$.

dx.doi.org/10.1021/jp510769p | J. Phys. Chem. B 2015, 119, 7266−7274

Solutions were spin-coated (Specialty Coating Systems P6700) onto clean glass coverslips to produce a thin polymer film, approximately 100−200 nm thick. Confocal single-molecule measurements were performed either on the microscope described above with the sample mounted on an $x-y$ piezo stage, (Physik Instrumente P-517) or on a similar microscope described elsewhere.[24] A clean, blank slide was used to measure the IRF for analysis of single-molecule fluorescence lifetimes. Single-molecule trajectories and fluorescence lifetimes were determined using the BIFL software package (Scientific Software Technologies Center). Further details of the instrument, data collection, and analysis procedures have been outlined previously.[25] Wide-field single-molecule images were recorded on an inverted single-molecule microscope described previously.[26] Defocused images were obtained by moving the objective toward the sample by ∼1 μm, revealing the angular distribution of emitted light intensity.[27,28] The patterns observed are a function of the emission dipole orientation and can be related to molecular orientation as well as indicate whether the image is from a single dipole emitter. The defocused image patterns were matched to theoretical patterns calculated as described elsewhere.[29,30]

RESULTS AND DISCUSSION

Donor−acceptor block copolymers must have appropriate energy levels and redox properties to allow for effective charge transfer; in this case, from the electron donor PFM block to the F8BT acceptor block.[31] Figure 1 shows the absorption

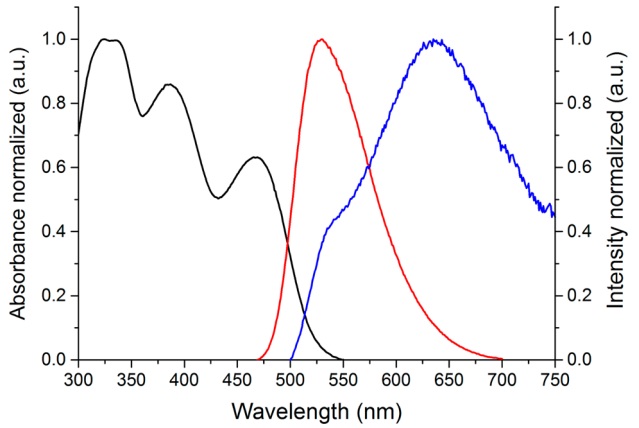

Figure 1. Absorption and emission spectra of PFM-F8BT-PFM. The absorption spectrum is measured in toluene; emission spectra are measured in toluene (red) and as a neat film (blue), (λ_{exc} = 470 nm).

spectrum of the block copolymer in toluene solution, and it features three distinct but overlapping absorption bands with wavelength maxima at approximately 330, 390, and 470 nm. The shape of the PFM-F8BT-PFM absorbance spectrum can be described by the sum of the absorbance spectra of the two homopolymer blocks that comprise the copolymer (Figure 1 in the Supporting Information) with assignment of the bands as follows: the 300 and 470 nm bands are associated with absorption by the F8BT block and the 390 nm band with PFM absorption. The solution absorbance spectra of the homopolymers correspond well to spectra reported elsewhere.[32,33]

Fluorescence emission from all of PFM, F8BT, and PFM-F8BT-PFM shows a shift to lower energy with increasing solvent polarity (Figure 2 and Table 1 in the Supporting Information). F8BT undergoes a red-shift of 37 nm (1300 cm^{-1}), from 512 nm in cyclohexane to 549 nm in benzonitrile, whereas for PFM, a much larger shift of 95 nm (4100 cm^{-1}) occurs on going from cyclohexane to dichloromethane (PFM not being soluble in benzonitrile). The shape of the emission spectrum also changes with the polarity of the solvent. PFM emission in cyclohexane is narrow and shows some vibronic structure but becomes increasingly broad and red-shifted as the solvent polarity increases. This large solvatochromic effect is consistent with reports of other polyfluorenes.[19,34] PFM-F8BT-PFM shows some difference in solvatochromism depending on the excitation wavelength. When the PFM block is excited at 380 nm (the selectivity over F8BT at this wavelength is approximately 8:1), the PFM-F8BT-PFM copolymer shows mostly PFM-like emission in cyclohexane with some F8BT emission. The proportion of F8BT emission increases in toluene, and in the more polar solvent $CHCl_3$ primarily F8BT-like emission is observed, as is the case when solvents of even higher polarity are used. When PFM-F8BT-PFM is excited at 460 nm (F8BT is excited almost exclusively at this wavelength), the emission spectrum is associated with F8BT, as expected.

Changing the polarity of the solvent also affects the fluorescence quantum yield of PFM-F8BT-PFM. In toluene, the polymer shows a fluorescence quantum yield of 0.38, which drops significantly to 0.17 in $CHCl_3$. The stabilization of an available charge-transfer state,[35,36] which may form at the interface between donor and acceptor blocks, is the likely reason for the increase in the nonradiative decay in the more polar solvent leading to the decrease in the fluorescence quantum yield. Photoinduced absorption spectroscopy has shown some evidence of the formation of a charge-transfer state following photoexcitation of the PFM block for the copolymer; however, the transient spectra were dominated by triplet state transient absorptions.[20]

The emission spectrum of a neat PFM-F8BT-PFM film is also shown in Figure 1. The neat film shows a very different emission spectrum compared to solution spectra and comprises a broad, red-shifted emission in the 600−700 nm range as well as some F8BT-like emission at 550 nm. The red-shifted emission is consistent with reports that PFM-F8BT-PFM forms an exciplex in the bulk state.[20] The lack of red-shifted emission in solution suggests that emissive exciplex formation requires close interchain interactions.

Time-Resolved Measurements. Figure 2a shows the fluorescence decay profile of the homopolymer F8BT in toluene solution and neat film. In toluene, F8BT decays monoexponentially with a fluorescence lifetime of 2.2 ns while in neat film its decay is more complex with a second, shorter-lifetime component present contributing the bulk of the light emitted. This suggests that in a solid film, environmental heterogeneity and interchain interactions affect the majority of the excited F8BT chromophores such that the fluorescence detected decays on a much shorter time scale. A small portion of the F8BT chromophores in the film, however, emit with a similar decay time (2.2 ns) as in solution. Figure 2b shows the fluorescence decay of PFM-F8BT-PFM, excited at 488 nm. Interestingly, in toluene, a biexponential decay function is required and in film, the decay requires the sum of four exponential terms to achieve satisfactory fitting, indicating that additional relaxation pathways, compared to F8BT, contribute to the observed emission in both solution and neat film. As seen for F8BT film, there is a fast subnanosecond component in neat film of the copolymer, attributable to interchain interactions. As mentioned above, there is the possibility for the

dx.doi.org/10.1021/jp510769p | J. Phys. Chem. B 2015, 119, 7266−7274

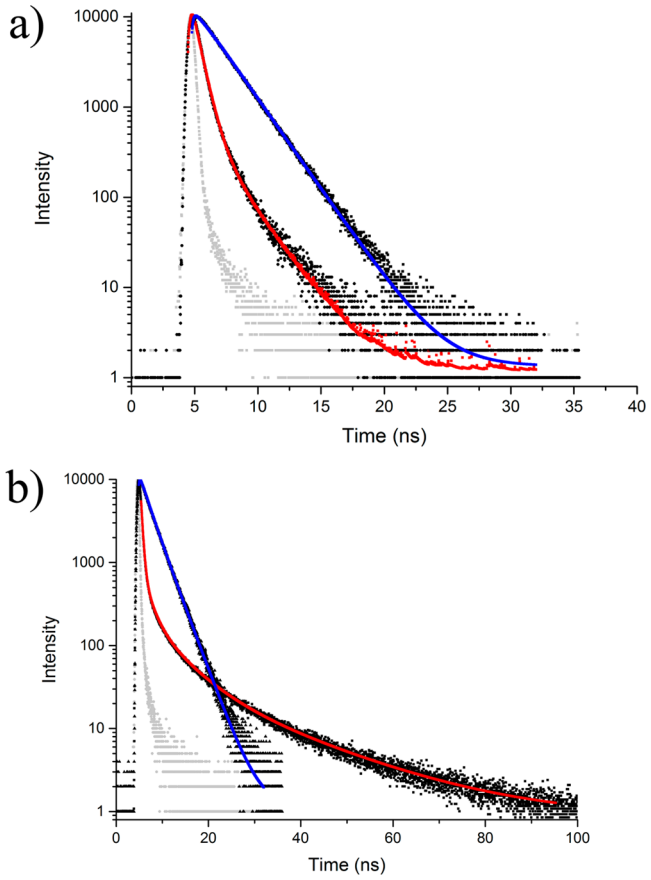

Figure 2. Fluorescence decays (black data points) and fitted functions (colored lines) of (a) F8BT and (b) PFM-F8BT-PFM in toluene (blue) and neat film (red). Excitation was at 488 nm with emission detected at 560 nm. The instrument response function is shown in gray.

locally excited state to form an excited state donor−acceptor complex (exciplex) with an adjacent chain where the interacting species meet the geometric requirements. This can occur in bulk films where PFM blocks can stack with the F8BT blocks from nearby chains. The longest lifetime in neat film (τ_4 = 19 ns) is attributed to these intermolecular states. The fitted parameters for all these samples are given in Table 1.

In addition to the formation of excited-state complexes, donor−acceptor copolymers are capable of intramolecular charge transfer at the interface between the donor and acceptor blocks.[12,31,35−38] The charge-transfer state for the closely related donor−acceptor pair, PFB and F8BT, has been estimated at 1.93 eV, using the methods outlined by Janssen et al.[35] The complex fluorescence decay kinetics observed in the present system suggests that a charge-transfer state is also available and accessible from the locally excited (LE) state of F8BT.[31] The usual fate of charge-transfer states is charge recombination to reform the ground state nonradiatively, although it is possible for this to be a radiative relaxation via charge-transfer emission. In rare circumstances where the energy levels are appropriately well matched and the LE and CT states suitably coupled, the LE-CT equilibrium can lead to a delayed fluorescence. Figure 3 shows the kinetic scheme for

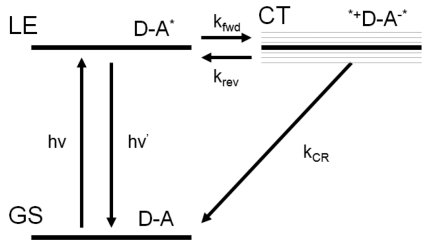

Figure 3. Kinetic scheme describing the interaction between the ground (GS), locally excited (LE), and charge-transfer (CT) states for the donor−acceptor (D-A) block copolymer. The LE state is depicted with the acceptor excited because in the majority of these measurements, it is F8BT which is photoexcited. The fainter lines above and below the CT state indicate the variation of the energy of the CT state with polarity.

such a situation. An equilibrium is established between the LE state and the CT state, and two fluorescence lifetimes are observed: a shorter fluorescence decay associated with quenching of the excited state by CT and a longer decay component arising following thermal regeneration of the LE state. When the CT state is nonemissive, any emission observed has the spectral characteristics of the LE state. For the triblock copolymer under investigation here, the F8BT-like emission spectrum observed and the nonsingle exponential decay kinetics are consistent with a delayed fluorescence. In toluene solution, fluorescence emission is characteristic of F8BT and the two decay components can be associated with forward CT (1.5 ns) and reverse CT (thermal regeneration of LE) (2.9 ns), respectively. In neat film, there is the added complication of the much faster (sub-nanosecond) component due to interchain interactions as seen for F8BT alone. A delayed fluorescence is clearly observable with associated fluorescence components of 1.7 ns (forward CT) and 5.9 ns (reverse CT), respectively. Further evidence that emission is occurring from a state with characteristics similar to F8BT comes from Lippert−Mataga plots (Figure 3 in the Supporting Information) of the steady-state emission from PFM, F8BT, and PFM-F8BT-PFM. The nature of the excited state of PFM is clearly different from that of F8BT, whereas for the copolymer it is very similar to that of F8BT. If emission in the copolymer were from a CT state, a solvent polarity gradient very different from that of the F8BT state would be expected.

On the basis of the energy level scheme described in Figure 3, the rate constants and driving forces for the forward and reverse charge-transfer processes can be calculated (Table 2).[39] The rate constants of forward and reverse charge transfer between the LE and CT states (k_{fwd} and k_{rev}, respectively) and

Table 1. Fluorescence Decay Data for F8BT and PFM-F8BT-PFM in Toluene Solution and Neat Film

	F8BT		PFM-F8BT-PFM			
	τ_1 (ns)	τ_2 (ns)	τ_1 (ns)	τ_2 (ns)	τ_3 (ns)	τ_4 (ns)
toluene	2.2 (100)[a]	–	1.5 (23)	2.9 (77)	–	–
neat film	0.59 (84)	2.2 (16)	0.39 (34)	1.7 (27)	5.9 (19)	19 (20)

[a]The numbers in parentheses are the fractions of light emitted (as a percent) attributable to each component.

dx.doi.org/10.1021/jp510769p | J. Phys. Chem. B 2015, 119, 7266−7274

Table 2. Rate Constants and Related Parameters Derived for Charge Transfer in PFM-F8BT-PFM in Solution and Film (Rate Constants Defined in Figure 3)

	k_{fwd} ($\times 10^8$ s^{-1})	k_{rev} ($\times 10^8$ s^{-1})	k_{CR} ($\times 10^8$ s^{-1})	K_{eq}	ΔG_{CT} (eV)
toluene	0.7	4.0	1.6	0.17	0.045
neat film	1.2	2.1	0.3	0.58	0.014

the rate constant for charge recombination to the GS (k_{CR}) are calculated from the decay times (τ_i and τ_j) and pre-exponential factors (a_i and a_j) of the two decay components of the total fluorescence decay attributed to delayed fluorescence (i.e., those associated with the forward and reverse CT processes), and τ_0, the fluorescence lifetime of the unquenched acceptor (details of the calculations are provided in the Supporting Information). k_{fwd} and k_{rev} in toluene are found to be 6.8×10^7 s^{-1} and 4.0×10^8 s^{-1}, respectively. k_{CR} is slower than k_{rev} at 1.6×10^8 s^{-1}, indicating that the major pathway for CT relaxation is back through the LE state and not via recombination to the GS. These rate constants give an equilibrium constant (K_{eq}) between the LE and CT states of 0.17 and a driving force (ΔG_{CT}) of +0.045 eV from the LE to the CT state. This shows that the equilibrium favors slightly the LE state and that the initial charge-transfer process is energetically slightly unfavorable but that the CT state is still accessible at room temperature. The closeness in energy of the LE and CT states implies that the energy of the CT state in toluene is approximately 2.5 eV, taking the energy of the LE state as that where the normalized absorption and emission spectra intersect (503 nm, see Figure 1). This is consistent with the value mentioned above for the CT state of PFB-F8BT, which was obtained in *ortho*-dichlorobenzene. This solvent is moderately polar (ε_s ~10) and would lower the energy of the CT state compared to toluene. Delayed fluorescence is also apparent in neat film, and k_{fwd} and k_{rev} are calculated to be 1.2×10^8 and 2.1×10^8 s^{-1}, respectively, yielding a K_{eq} of 0.58 and ΔG_{CT} of 0.014 eV, indicating that CT is marginally more favored than in toluene. k_{CR}, however, in the neat film (3.4×10^7 s^{-1}) is considerably slower and less competitive than in solution, likely a result of the much more rigid nature of a neat film.

Single-Molecule Experiments. Figure 4 shows two confocal fluorescence trajectories obtained from individual PFM-F8BT-PFM chains in PMMA. The intensity of both molecules fluctuates over time, with counts rates early in the trajectories as high as 5000 and 12000 s^{-1} for the two chains. Both molecules show good photostability, emitting photons over minutes with the second molecule still emitting after 10 min of pulsed laser excitation. The fluorescence decay kinetics of the two molecules are strikingly different. The molecule shown in Figure 4a emits with monoexponential decay kinetics, whereas the molecule shown in Figure 4b is biexponential for the duration of its trajectory. These two molecules are essentially representative of the data set. Of the 149 PFM-F8BT-PFM chains measured, 137 showed either mono (72 molecules, 48%) or biexponential (65 molecules, 44%) kinetics for their entire trajectory, while the remaining 12 molecules (8%) showed periods of each type of decay kinetics (at least 20 000 photons or two adjacent data points). In contrast to this, single chains of the homopolymer F8BT (see Figure 4 in the Supporting Information for an example) show exclusively monoexponential decays (103 molecules examined).

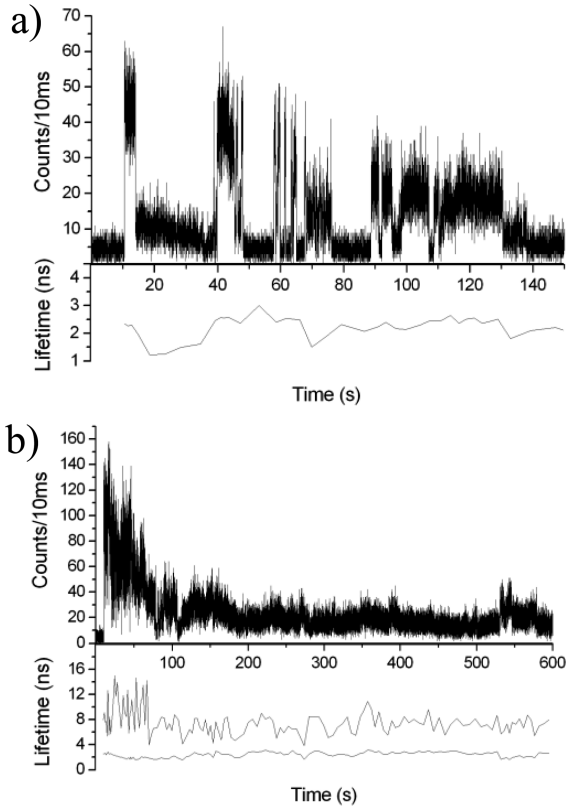

Figure 4. Fluorescence trajectories for two individual PFM-F8BT-PFM chains in PMMA showing (a) monoexponential and (b) biexponential fluorescence decay kinetics. For each molecule, the upper panel shows counts with time in 10 ms bins and the lower panel shows the fluorescence lifetime(s) calculated every 10 000 photons along the course of the trajectory.

Histograms showing the distributions of fluorescence lifetimes for F8BT and PFM-F8BT-PFM are shown in Figure 5. For histogram construction, a representative value for the lifetime(s) of each molecule was determined by averaging over the entire trajectory. For most molecules, the fluorescence lifetimes did not vary substantially over the course of the molecule's trajectory. This is particularly so for molecules showing monoexponential behavior, i.e., all F8BT molecules and approximately one-half of the PFM-F8BT-PFM molecules; therefore, a representative value for the lifetime was straightforward to estimate and enter into the histograms in Figure 5a,b. The histograms in Figure 5c are built from molecules of PFM-F8BT-PFM showing biexponential kinetics with one histogram for each lifetime. The 12 molecules noted above that showed biexponential behavior for only a portion of their trajectory were included in the histograms in Figure 5c.

Figure 5a shows the distribution of lifetimes for F8BT and is centered around 2.3 ns. For the chains of PFM-F8BT-PFM that show monoexponential decay, it is centered around 2.6 ns. These values are very similar to the values obtained in toluene solution for these compounds. The other half of the PFM-F8BT-PFM chains measured show two distinct lifetimes: a shorter lifetime distributed quite tightly around 2.1 ns, and a longer-lived component with more widely varying lifetime in the range of ~6−12 ns.

The observation of biexponential decay kinetics from single chains of the copolymer is unusual because single molecules are expected to show a single emission pathway and therefore a

dx.doi.org/10.1021/jp510769p | J. Phys. Chem. B 2015, 119, 7266−7274

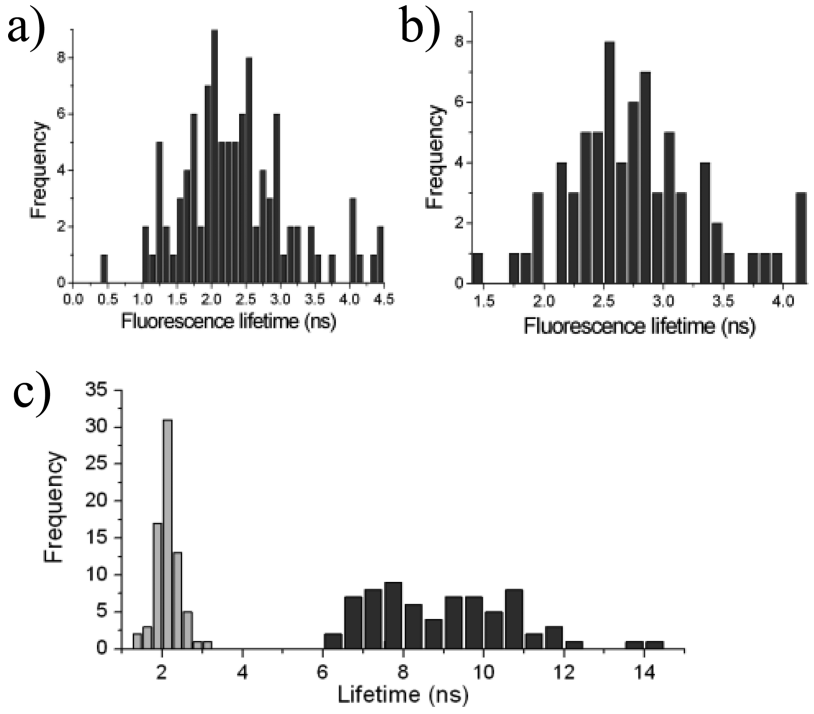

Figure 5. Distribution of fluorescence lifetimes from single chains in PMMA of (a) F8BT, (b) PFM-F8BT-PFM showing monoexponential decay kinetics, and (c) PFM-F8BT-PFM showing biexponential decay kinetics. The two histograms are of the two lifetimes extracted from biexponential fitting functions.

monoexponential decay. Two possible trivial explanations are poor dilution or contamination with another species resulting in two molecules within the confocal detection volume. These possibilities can be ruled out because half of the measured molecules show biexponential decay kinetics and no molecules have been recorded showing only a single, longer fluorescence lifetime. Another possibility is that because these molecules are ~30 kDa polymer chains, biexponential kinetics could arise from there being multiple emitting sites within a single chain. Defocused wide-field imaging of single chains of the PFM-F8BT triblock copolymer in PMMA (Figure 6) reveals emission patterns consistent with there being a single emitting site within each polymer chain for 93% of chains imaged (167 out of 179), ruling out multiple emission sites as the origin of biexponential kinetics observed in over 50% of single molecules studied by confocal microscopy.

A more likely explanation for the observed biexponential kinetics in single chains of PFM-F8BT-PFM, consistent with the ensemble solution and neat film results, is that the two fluorescence lifetimes in some chains arise from delayed fluorescence due to charge transfer at the donor−acceptor interface. Delayed fluorescence arising from an LE−CT equilibrium is relatively unusual and has been reported at the single-molecule level in only a few cases.[15,40] To our knowledge, this is the first example of delayed fluorescence in single chains of a donor−acceptor conjugated copolymer arising from this mechanism.

This interpretation is supported by concurrently recorded emission spectra (Figure 7) from single chains of PFM-F8BT-PFM. Half of the emitted fluorescence was directed to a CCD camera and an emission spectrum recorded every 5 s. There is no red-shifting of the emission in PFM-F8BT-PFM compared to F8BT, i.e. F8BT-like spectra were recorded for all 149 PFM-F8BT-PFM molecules studied whether they showed mono- or

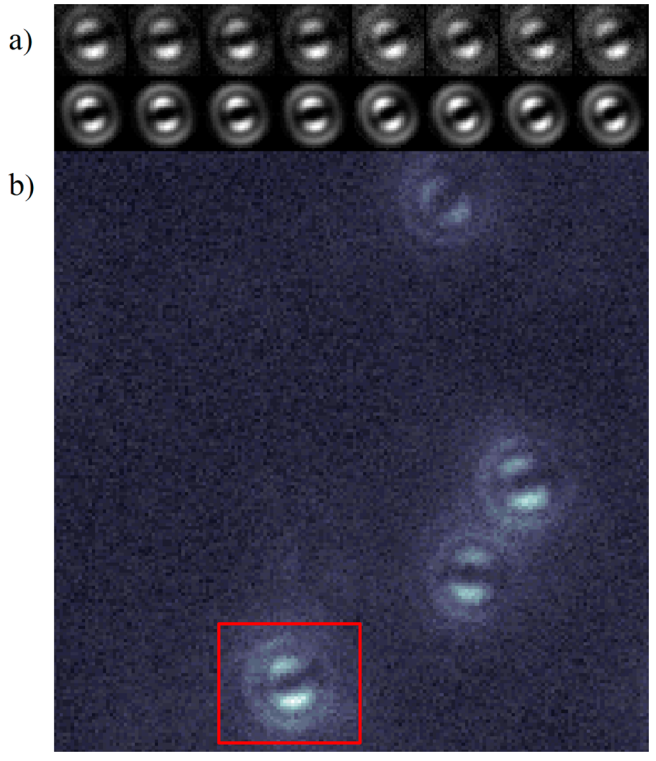

Figure 6. (a) Defocused wide-field images (upper panels) of a single PFM-F8BT-PFM molecule in PMMA with fitted patterns (lower panels) indicative of a single emitter. (b) Defocused wide-field image of 4 single molecules of PFM-F8BT in PMMA with the molecule examined in panel a indicated. Integration time, 5 s; excitation, 470 nm.

dx.doi.org/10.1021/jp510769p | J. Phys. Chem. B 2015, 119, 7266−7274

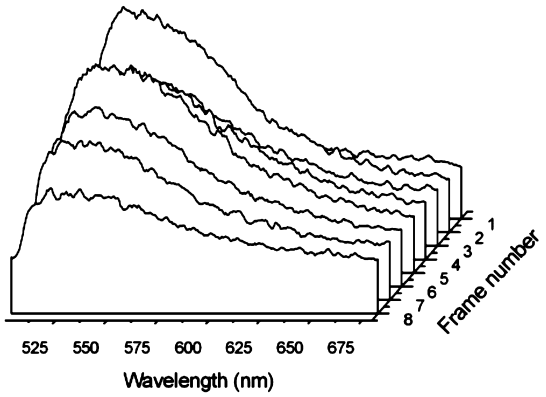

Figure 7. Emission spectra (integration time, 5 s/spectrum) collected from a single, isolated chain of PFM-F8BT-PFM in a PMMA film. The molecule studied here displayed biexponential decay kinetics.

biexponential decay kinetics. Although it is known that these polymers form exciplexes in the bulk state and some emission consistent with this was observed from a neat film of the copolymer, it is unlikely that these are formed at the single-molecule level. Intrachain exciplexes with the required overlapped geometry would require stacking of the donor and acceptor blocks via chain folding. However, these block copolymers are rigid, making this degree of chain collapse unlikely.

Using the same procedure adopted for bulk solution and neat film data, the rate constants and kinetic parameters for CT can be calculated from the time-resolved single-molecule data. Taking representative values for decay constants and pre-exponential factors from the biexponential single-molecule trajectory shown in Figure 4b, the forward and reverse rate constants (k_{fwd} and k_{rev}) were found to be 7.3×10^7 s^{-1} and 1.5×10^8 s^{-1}, respectively, with a nonradiative rate constant for recombination from the CT state to the GS (k_{CR}) of 2×10^5 s^{-1}. This process is not competitive with the forward and reverse rate constants for the majority of the molecules measured, indicating that few excitations are lost through charge recombination from the charge-transfer state back to the ground state. The equilibrium constant (K_{eq}) of 0.50, and driving force (ΔG) of 0.018 eV are comparable with the values calculated from the solution and neat film samples. For the molecules which show only monoexponential decay kinetics, it may be that, because of local environment and chain conformation differences, the charge-transfer state energy is too high and forward CT is noncompetitive with other radiative and nonradiative relaxation processes.

The distribution of single-molecule behaviors is likely a result of the energy of the charge-transfer state being dependent on the local environment and polarity in the film. Furthermore, this raises the possibility that the local environment can fluctuate over time as well. Evidence for this can be seen in changes in the behavior of a single molecule over time, such as the one shown in Figure 8. This molecule shows evidence of both mono- and biexponential decays. At first, the CT state is unavailable and emission intensity (Figure 8a) is high and the kinetics are monoexponential with a lifetime (Figure 8b) of 3.2 ns. From 23 to 63 s, the intensity is greatly reduced and the decay kinetics become biexponential (with lifetimes of 1.4 and 7.1 ns), indicating that the CT state can now be accessed following excitation. This situation endures for ~30 s, after which the CT state becomes unavailable and the decay

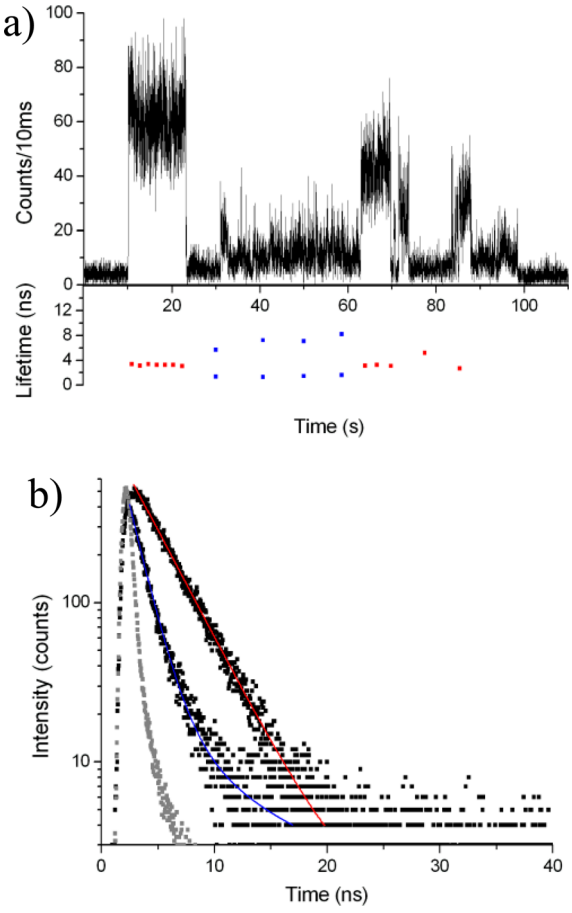

Figure 8. (a) Fluorescence trajectory of an isolated PFM-F8BT-PFM chain in PMMA showing a change from single to biexponential fluorescence decay and (b) example fluorescence decay profiles constructed from photons in the 15−18 s range and fitted by a single exponential decay (red) and from photons in the 40−50 s range and fitted by a biexponential decay (blue).

becomes monoexponential again. For molecules in a PMMA host matrix, polymer segmental motion can lead to changes in the local polarity that they experience.[41] As the energy of the CT state is affected by polarity, this may lead to the fluctuating availability of the CT state and hence the appearance of delayed fluorescence.

CONCLUSION

Donor−acceptor conjugated block copolymers are potentially useful materials for photovoltaic devices. In neat films, PFM-F8BT-PFM shows a broad, red-shifted emission typical of exciplexes, associated with a long fluorescence decay component. This exciplex emission is not found in solution or at the single-molecule level in solid films, although complex fluorescence decay dynamics remain. A delayed fluorescence is observed under these conditions that is attributed to a charge-transfer state that can form at the interface between the donor and acceptor. This type of delayed fluorescence, involving an equilibrium between the locally excited state and charge-transfer state, is unusual and observed here even at the single-chain level, highlighting the intrachain nature of the process. These results provide further insight into the complex photophysics that occurs in conjugated polymers and that is relevant to their applications as active materials in optoelectronic devices.

dx.doi.org/10.1021/jp510769p | J. Phys. Chem. B 2015, 119, 7266−7274

■ ASSOCIATED CONTENT

Supporting Information

Additional steady-state spectra and Lippert−Mataga plots for PFM, F8BT ,and PFM-F8BT-PFM; fluorescence quantum yields of PFM-F8BT; example SM trajectory and lifetimes plot for a F8BT molecule; kinetic equations for delayed fluorescence. This material is available free of charge via the Internet at http://pubs.acs.org.

■ AUTHOR INFORMATION

Corresponding Authors

*Tel.: +61 3 9905 4566. Fax: +61 3 9905 4597. E-mail: toby.bell@monash.edu.

*Tel.: +61 3 8344 8939. Fax: +61 3 9347 5180. E-mail: ghiggino@unimelb.edu.au.

Notes

The authors declare no competing financial interest.

■ ACKNOWLEDGMENTS

We thank the Australian Research Council (ARC) for financial support of this research through Grants DP0986166, LE100100131, and LE110100161. E.N.H. acknowledges an Australian Postgraduate Award. We acknowledge Sam Ashworth for technical assistance with data collection. N.C.G. is grateful to the School of Chemistry, The University of Melbourne for a Wilsmore Fellowship, and to Queen's College, Melbourne for a Sugden Fellowship.

■ REFERENCES

(1) Grimsdale, A. C.; Chan, K. L.; Martin, R. E.; Jokisz, P. G.; Holmes, A. B. Synthesis of Light-Emitting Conjugated Polymers for Applications in Electroluminescent Devices. *Chem. Rev. (Washington, DC, U.S.)* **2009**, *109*, 897−1091.

(2) Banal, J. L.; Subbiah, J.; Graham, H.; Lee, J.-K.; Ghiggino, K. P.; Wong, W. W. H. Electron Deficient Conjugated Polymers Based on Benzotriazole. *Polym. Chem.* **2013**, *4*, 1077−1083.

(3) Friend, R. H.; Gymer, R. W.; Holmes, A. B.; Burroughes, J. H.; Marks, R. N.; Taliani, C.; Bradley, D. D. C.; Dos Santos, D. A.; Bredas, J. L.; Logdlund, M.; et al. Electroluminescence in Conjugated Polymers. *Nature (London, U.K.)* **1999**, *397*, 121−128.

(4) Kippelen, B.; Brédas, J. L. Organic Photovoltaics. *Energy Environ. Sci.* **2009**, *2*, 251−261.

(5) Li, C.; Liu, M.; Pschirer, N. G.; Baumgarten, M.; Müllen, K. Polyphenylene-Based Materials for Organic Photovoltaics. *Chem. Rev. (Washington, DC, U.S.)* **2010**, *110*, 6817−6855.

(6) Arias, A. C.; MacKenzie, J. D.; Stevenson, R.; Halls, J. J. M.; Inbasekaran, M.; Woo, E. P.; Richards, D.; Friend, R. H. Photovoltaic Performance and Morphology of Polyfluorene Blends: A Combined Microscopic and Photovoltaic Investigation. *Macromolecules* **2001**, *34*, 6005−6013.

(7) Hoppe, H.; Sariciftci, N. S. Morphology of Polymer/Fullerene Bulk Heterojunction Solar Cells. *J. Mater. Chem.* **2006**, *16*, 45−61.

(8) Mulherin, R. C.; Jung, S.; Huettner, S.; Johnson, K.; Kohn, P.; Sommer, M.; Allard, S.; Scherf, U.; Greenham, N. C. Ternary Photovoltaic Blends Incorporating an All-Conjugated Donor-Acceptor Diblock Copolymer. *Nano Lett.* **2011**, *11*, 4846−4851.

(9) Bicciocchi, E.; Chen, M.; Rizzardo, E.; Ghiggino, K. P. Synthesis of a Rod-Coil Copolymer Incorporating PCBM. *Polym. Chem.* **2012**, *4*, 53−56.

(10) Guo, C.; Lin, Y.-H.; Witman, M. D.; Smith, K. A.; Wang, C.; Hexemer, A.; Strzalka, J.; Gomez, E. D.; Verduzco, R. Conjugated Block Copolymer Photovoltaics with Near 3% Efficiency through Microphase Separation. *Nano Lett.* **2013**, *13*, 2957−2963.

(11) Sommer, M.; Huettner, S.; Thelakkat, M. Donor-Acceptor Block Copolymers for Photovoltaic Applications. *J. Mater. Chem.* **2010**, *20*, 10788−10797.

(12) Morteani, A. C.; Sreearunothai, P.; Herz, L. M.; Friend, R. H.; Silva, C. Exciton Regeneration of Polymeric Semiconductor Heterojunctions. *Phys. Rev. Lett.* **2004**, *92*, 247402.

(13) Morteani, A. C.; Dhoot, A. S.; Kim, J.-S.; Silva, C.; Greenham, N. C.; Murphy, C.; Moons, E.; Ciná, S.; Burroughes, J. H.; Friend, R. H. Barrier-Free Electron-Hole Capture in Polymer Blend Heterojunction Light-Emitting Diodes. *Adv. Mater. (Weinheim, Ger.)* **2003**, *15*, 1708−1712.

(14) Higginbotham, H. F.; Cox, R. P.; Sandanayake, S.; Graystone, B. A.; Langford, S. J.; Bell, T. D. M. A Fluorescent "2 in 1" Proton Sensor and Polarity Probe Based on Core Substituted Naphthalene Diimide. *Chem. Commun. (Cambridge, U.K.)* **2013**, *49*, 5061−5063.

(15) Bell, T. D. M.; Stefan, A.; Masuo, S.; Vosch, T.; Lor, M.; Cotlet, M.; Hofkens, J.; Bernhardt, S.; Muellen, K.; Van der Auweraer, M.; et al. Electron Transfer at the Single Molecule Level in a Triphenylamine-Perylene Imide Molecule. *ChemPhysChem* **2005**, *6*, 942−948.

(16) Barbara, P. F.; Meyer, T. J.; Ratner, M. A. Contemporary Issues in Electron Transfer Research. *J. Phys. Chem.* **1996**, *100*, 13148−13168.

(17) Redecker, M.; Bradley, D. D. C.; Inbasekaran, M.; Wu, W. W.; Woo, E. P. High Mobility Hole Transport Fluorene-Triamine Copolymers. *Adv. Mater. (Weinheim, Ger.)* **1999**, *11*, 241−246.

(18) Petrozza, A.; Laquai, F.; Howard, I. A.; Kim, J.-S.; Friend, R. H. Dielectric Switching of the Nature of Excited Singlet State in a Donor-Acceptor-Type Polyfluorene Copolymer. *Phys. Rev. B: Condens. Matter Mater. Phys.* **2010**, *81*, 205421.

(19) Dias, F. B.; King, S.; Monkman, A. P.; Perepichka, I. I.; Kryuchkov, M. A.; Perepichka, I. F.; Bryce, M. R. Dipolar Stabilization of Emissive Singlet Charge Transfer Excited States in Polyfluorene Copolymers. *J. Phys. Chem. B* **2008**, *112*, 6557−6566.

(20) Yan, C.; Cadby, A. J.; Parnell, A. J.; Tang, W.; Skoda, M. W. A.; Mohamad, D.; King, S. P.; Reynolds, L. X.; Haque, S. A.; Wang, T.; et al. Photophysics and Morphology of a Polyfluorene Donor-Acceptor Triblock Copolymer for Solar Cells. *J. Poly. Sci., Part B: Polym. Phys.* **2013**, *51*, 1705−1718.

(21) Holmes, A.; Jones, D.; Wong, W. H. W.; Haque, S. Conjugated block copolymers, methods of preparation and their use in heterojunction devices. PCT Int. Appl., WO 2010060159 A1 20100603, 2010.

(22) Kellogg, R. E.; Bennett, R. G. Radiationless Intermolecular Energy Transfer. III. Determination of Phosphorescence Efficiencies. *J. Chem. Phys.* **1964**, *41*, 3042−3045.

(23) Cox, R. P.; Higginbotham, H. F.; Graystone, B. A.; Sandanayake, S.; Langford, S. J.; Bell, T. D. M. A New Fluorescence H^+ Sensor Based on Core-Substituted Naphthalene Diimide. *Chem. Phys. Lett.* **2012**, *521*, 59−63.

(24) Gomez, D. E.; Tan, T. A. T.; White, J. M.; Bell, T. D. M.; Ghiggino, K. P. Synthesis and Single Chain Fluorescence of a Sulfonated Conjugated Polymer. *Aust. J. Chem.* **2009**, *62*, 1577−1582.

(25) Bell, T. D. M.; Yap, S.; Jani, C. H.; Bhosale, S. V.; Hofkens, J.; De Schryver, F. C.; Langford, S. J.; Ghiggino, K. P. Synthesis and Photophysics of Core-Substituted Naphthalene Diimides: Fluorophores for Single Molecule Applications. *Chem.—Asian J.* **2009**, *4*, 1542−1550.

(26) Hooley, E. N.; Tilley, A. J.; White, J. M.; Ghiggino, K. P.; Bell, T. D. M. Energy Transfer in PPV-Based Conjugated Polymers: A Defocused Widefield Fluorescence Microscopy Study. *Phys. Chem. Chem. Phys.* **2014**, *16*, 7108−7114.

(27) Patra, D.; Gregor, I.; Enderlein, J. Image Analysis of Defocused Single-Molecule Images for Three-Dimensional Molecule Orientation Studies. *J. Phys. Chem. A* **2004**, *108*, 6836−6841.

(28) Böhmer, M.; Enderlein, J. Orientation Imaging of Single Molecules by Wide-Field Epifluorescence Microscopy. *J. Opt. Soc. Am. B* **2003**, *20*, 554−559.

(29) Dedecker, P.; Muls, B.; Deres, A.; Uji-i, H.; Hotta, J.; Sliwa, M.; Soumillion, J.; Müllen, K.; Enderlein, J.; Hofkens, J. Defocused Wide-Field Imaging Unravels Structural and Temporal Heterogeneity in Complex Systems. *Adv. Mater. (Weinheim, Ger.)* **2009**, *21*, 1079−1090.
(30) Uji-i, H.; Melnikov, S. M.; Deres, A.; Bergamini, G.; De Schryver, F.; Herrmann, A.; Müllen, K.; Enderlein, J.; Hofkens, J. Visualizing Spatial and Temporal Heterogeneity of Single Molecule Rotational Diffusion in a Glassy Polymer by Defocused Wide-Field Imaging. *Polymer* **2006**, *47*, 2511−2518.
(31) Bittner, E. R.; Ramon, J. G. S.; Karabunarliev, S. Exciton Dissociation Dynamics in Model Donor-Acceptor Polymer Heterojunctions. I. Energetics and Spectra. *J. Chem. Phys.* **2005**, *122*, 214719.
(32) Stevens, M. A.; Silva, C.; Russell, D. M.; Friend, R. H. Exciton Dissociation Mechanisms in the Polymeric Semiconductors Poly(9,9-dioctylfluorene) and Poly(9,9-dioctylfluorene-co-benzothiadiazole). *Phys. Rev. B: Condens. Matter Mater. Phys.* **2001**, *63*, 165213.
(33) Palilis, L. C.; Lidzey, D. G.; Redecker, M.; Bradley, D. D. C.; Inbasekaran, M.; Woo, E. P.; Wu, W. W. High Performance Blue Light-Emitting Diodes Based on Conjugated Polymer Blends. *Synth. Met.* **2001**, *121*, 1729−1730.
(34) Wu, W. C.; Liu, C. L.; Chen, W. C. Synthesis and Characterization of New Fluorene-Acceptor Alternating and Random Copolymers for Light-Emitting Applications. *Polymer* **2006**, *47*, 527−538.
(35) Janssen, A. J.; Veldman, B. D.; Meskers, S. C. J. The Energy of Charge-Transfer States in Electron Donor-Acceptor Blends: Insight into the Energy Losses in Organic Solar Cells. *Adv. Funct. Mater.* **2009**, *19*, 1939−1948.
(36) Huang, Y.-S.; Westenhoff, S.; Avilov, I.; Sreearunothai, P.; Hodgkiss, J. M.; Deleener, C.; Friend, R. H.; Beljonne, D. Electronic Structures of Interfacial States Formed at Polymeric Semiconductor Heterojunctions. *Nat. Mater.* **2008**, *7*, 483−489.
(37) Ramon, J. G. S.; Bittner, E. R. Exciton Regeneration Dynamics in Model Donor-Acceptor Polymer Heterojunctions. *J. Phys. Chem. B* **2006**, *110*, 21001−21009.
(38) Gelinas, S.; Pare, O.; Nadeau-Brosseau, C.; Albert-Seifried, S.; Mcneill, C. R.; Kirov, K. R.; Howard, I. A.; Leonelli, R.; Friend, R. H.; Silva, C. The Binding Energy of Charge-Transfer Excitons Localized at Polymeric Semiconductor Heterojunctions. *J. Phys. Chem. C* **2011**, *115*, 7114−7119.
(39) Gronheid, R.; Stefan, A.; Cotlet, M.; Hofkens, J.; Qu, J.; Müllen, K.; Van der Auweraer, M.; Verhoeven, J. W.; De Schryver, F. C. Reversible Intramolecular Electron Transfer at the Single-Molecule Level. *Angew. Chem., Int. Ed.* **2003**, *42*, 4209−4214.
(40) Cotlet, M.; Masuo, S.; Luo, G.; Hofkens, J.; Van der Auweraer, M.; Verhoeven, J.; Müllen, K.; Xie, X. S.; De Schryver, F. C. Probing Conformational Dynamics in Single Donor-Acceptor Synthetic Molecules by Means of Photoinduced Reversible Electron Transfer. *Proc. Natl. Acad. Sci. U.S.A.* **2004**, *101*, 14343−14348.
(41) Izquierdo, M. A.; Bell, T. D. M.; Habuchi, S.; Fron, E.; Pilot, R.; Vosch, T.; De Feyter, S.; Verhoeven, J.; Jacob, J.; Müllen, K.; et al. Switching of the Fluorescence Emission of Single Molecules Between the Locally Excited and Charge Transfer States. *Chem. Phys. Lett.* **2005**, *401*, 503−508.